Journal of
Environmental
Nanotechnology

Investigation on Pure and Aluminium Doped Hydroxyapatite for Orthopedic Applications

V. Kalaiselvi*, T. Loganayaki, M. Nathiya
Department of Physics, Navarasam Arts & Science College for Women, Arachalur, Erode, TN, India
Received: 28.01.2021 Accepted: 03.03.2021
*nk.arthikalai@gmail.com

ABSTRACT

Hydroxyapatite is the main nano biomaterial used in the field of orthopedic applications. In the present work synthesis and characterization of pure and doped Hydroxyapatite, nanoparticles were performed. Biomaterials were selected for the present study in view of their bone replacement applications. The main proposition of this work is to synthesize the Hydroxyapatite (Hap) nanoparticles by microwave-assisted co-precipitation method under room temperature. The prepared samples are characterized by using various techniques such as powder XRD, SEM, EDAX, UV-Visible, PL and FT-IR method. The antimicrobial analysis was performed to study the crystalline size, micro strain and dislocation density of the samples. SEM reveals the morphology of the samples. The composition of the samples was revealed by EDAX, UV, and PL reveal the optical property of the samples. Functional groups are determined by FTIR. Zone of inhibition for gram-positive and gram-negative bacteria was shown by antimicrobial analysis.

Keywords: EDAX; FT-IR; Hydroxyapatite; Nanomaterials; SEM; UV-Visible; XRD.

1. INTRODUCTION

This Calcium phosphates come under the community of ceramic material, which is widely used to treat orthopedic defects. Especially, Hydroxyapatite based ceramic material is considered as one of the potential calcium–phosphate candidate for bone and bone-related clinical applications because of their chemical composition that is closely related to that of the mineral phase of bone (Amogh Tathe *et al.* 2014; Vignesh Raj *et al.* 2018).

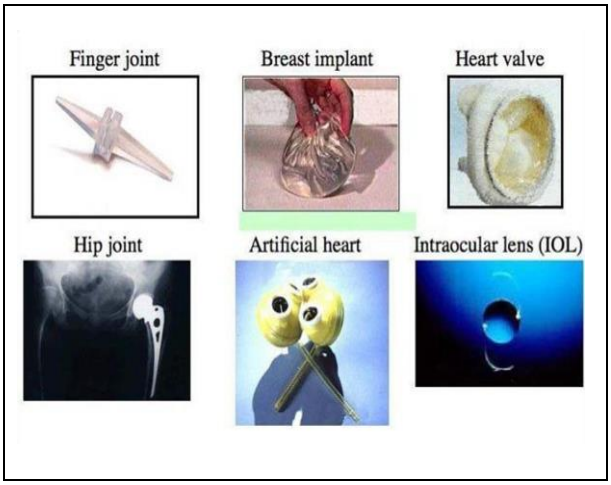

Fig. 1: Common Medical Devices Comprised of Biomaterials

However, many physical and mechanical properties of hydroxyapatite, including bioactivity, biocompatibility, solubility, sinterability, castability, fracture toughness and absorption, can be tailored over wide ranges by controlling the particle composition, size and morphology. Hence it is of great importance to developing synthesis methods focused on the precise control of particle size, morphology and chemical composition of Hydroxyapatite. Nowadays, the metal doped Hydroxyapatite particles with nanoscale level have a great impact since their small size and large specific surface area enable homogeneous resorption by osteoclasts (Gopi *et al.* 2012; Rajendran *et al.* 2014).

So in this present work, synthesis and characterization of pure and Al doped HAp nanoparticles were performed. These materials were selected for the present study in view of their bone replacement applications. The main proposition of this work is to synthesize the HAp nanoparticles by microwave-assisted co-precipitation method under room temperature. The prepared samples are characterized by using various techniques such as powder XRD, SEM, EDAX, UV-Visible, PL, FT-IR and Antimicrobial method. The antimicrobial analysis was performed to study the in-vitro analysis of the samples (Kanimozhi et al. 2014; Kalaiselvi et al. 2017).

2. MATERIALS & METHODS

2.1 Synthesis of HAp Nanoparticle

HAp nanoparticles were prepared by microwave irradiation method. 1 M of calcium hydroxide, 0.6M of orthophosphoric acid, capping agent 0.3M of Triethonalamine was dissolved in 100 ml of distilled water with stirring at room temperature for 1 hour. The H_3PO_4 was added with drop by drop in $Ca(OH)_2$ solution at room temperature. The capping agent is added to the mixture of $Ca(OH)_2$ and H_3PO_4 solution. Ammonia solution was added dropwise to the mixture, with constant stirring. This mixture was continuously stirred for 6 hours. These final products were allowed to cool for 24 hours with the help of an ice cube. This aged precipitate is washed with distilled water. Finally, white product was kept in a microwave oven at 70°C for 15 to 20 minutes. The dried sample was grained in a mortar and pestle to get white colour HAp nanopowder.

2.2 Synthesis of Aluminium Doped HAp Nanoparticle

Aluminium doped HAp nanoparticles were prepared by microwave irradiation method. 0.9 mol of $Ca(OH)_2$, 0.6 mol of H_3PO_4, capping agent 0.3 mol of TEA, 0.1 mol of Aluminium was dissolved in 100ml of distilled water under stirring at room temperature for 1 hour separately. The H_3PO_4 and aluminium solution was added drop by drop in calcium hydroxide solution at room temperature. And then, the capping agent is added to the mixture of $Ca(OH)_2$, H_3PO_4 and aluminium solution. Ammonia solution was added dropwise to the mixture, under stirring. This mixture was continuously stirred for 6 hours at room temperature. These final products were allowed to cool for 24 hours using an ice cube. This aged precipitate is washed with distilled water. Finally, the white product was kept in a microwave oven at 70°C for 15 to 20 minutes. The dried sample was grained in a mortar and pestle to get white colour Al-doped HAp nano powder.

3. RESULTS & DISCUSSION

3.1 XRD

The XRD analysis of the prepared sample of pure HApand Al-doped HApnanoparticles was done by powder –Ray diffraction using CuKα as X-Ray Source (λ=1.5406Aº). Fig. 2 represents the X-ray diffraction pattern of pure and Al-doped HAp nanoparticles. From fig. it was revealed that some major peaks emerge, which indicates the crystal form. HAp possess a polycrystalline structure. The strong diffraction peaks in the XRD spectrum of pure and Al-doped HAp nanoparticles occurring at 2θ values 10.5º, 25.8º, 32.1º, 32.8º, 34º and 49.6º are indexed as the (100), (002), (112), (300), (202), (213) crystal planes and correspond to the Hexagonal structure of HAp with lattice constant a=9.42Aº and c=6.879Aº which is consistent with the standard [JCPDS (74-566)] data. No other impurity peaks were detected. The obtained nanoparticles as phase pure. The absence of any peak from Aluminium confirms that Al acts as a substitutional dopant. A slight broadening and decrease in the maximum intensity of the peaks are noticed by adding Al dopant in the Hap lattice. The average grain size of the nanoparticles can be calculated using Debye-Scherrer's formula,

$$D=K\lambda/\beta\cos\theta$$

Where,

'D' is the mean crystallite size,
'K' is the shape factor taken as 0.9,
'λ' is the wavelength of monochromatic X-Ray beam(nm),
'β' is the FWHM (full width at half maximum) for the diffraction peak under consideration (in radians), and 'ɵ' is the diffraction angle (º).

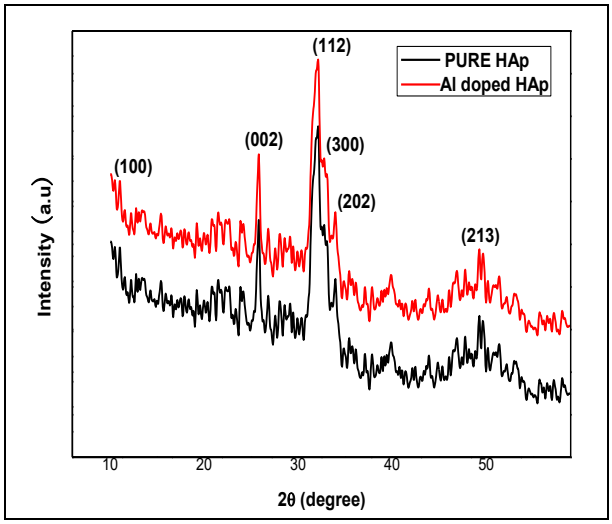

Fig. 2: XRD Patterns of Pure and Al-doped HAp Nanoparticles

Table 1. The crystalline size for pure HAp nanoparticles

Sample	2θ (deg.)	Crystalline size D(nm)	Average crystalline size (nm)
Pure HAp	10.5228	59.0814	35-67
	25.8210	24.7808	
	32.1206	63.3882	
	32.7789	66.9446	
	33.9691	38.9917	
	49.6207	35.1805	

Al-doped HAp	10.5233	55.9851	35-77
	25.8213	24.2424	
	32.1213	73.0521	
	32.7684	77.4670	
	33.9713	37.9573	
	49.6739	35.1557	

The Micro strain of the Hap nanoparticles is determined by the formula,

$$E_{strin} = \beta / 4 \tan \theta$$

Where,

'β' is the full width at half maximum for the diffraction peak (002) (in radians),

'ɵ' is the diffraction angle(°) for the peak (002).

The Dislocation density of the Hap nanoparticles is determined by the formula,

$$\delta = 1/D^2$$

Where,

'D' is the crystalline size in nm

Table 2. Micro Strain and Dislocation Density for Pure and Al-doped HAp

Sample	2θ	hkl	E_{strin} x 10^{-3}	Dislocation density δ x 10^{15}
Pure HAp	25.8°	(002)	6.25817	1.628
Al-doped HAp	25.8°	(002)	6.40856	1.701

The microstrain, as well as the dislocation density, is increased with the addition of dopant Al into the pure HAp nanoparticles.

3.2 SEM Analysis

The Morphology and crystallite size of the particles were investigated by SEM. The SEM image of the HAp nanoparticles corresponding to the XRD pattern in fig. 3 is shown in figure (a), it is clear that the prepared HAp nanoparticles have a spherical shape and uniform size with an average size varies from 52-66nm.

SEM demonstrates the non-homogeneity of the nanosized Al-doped HAp particles are seen as non-uniform agglomerates of elongated, spherical shapes and plate type shapes it is shown in figure (b). The particles size varies from 61-90nm.

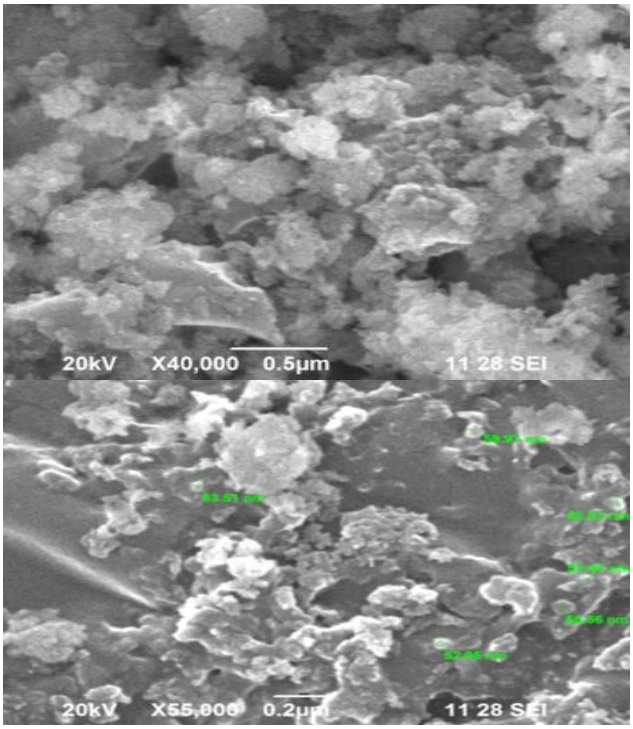

Fig. 3 (a): SEM images of pure HAp nanoparticles

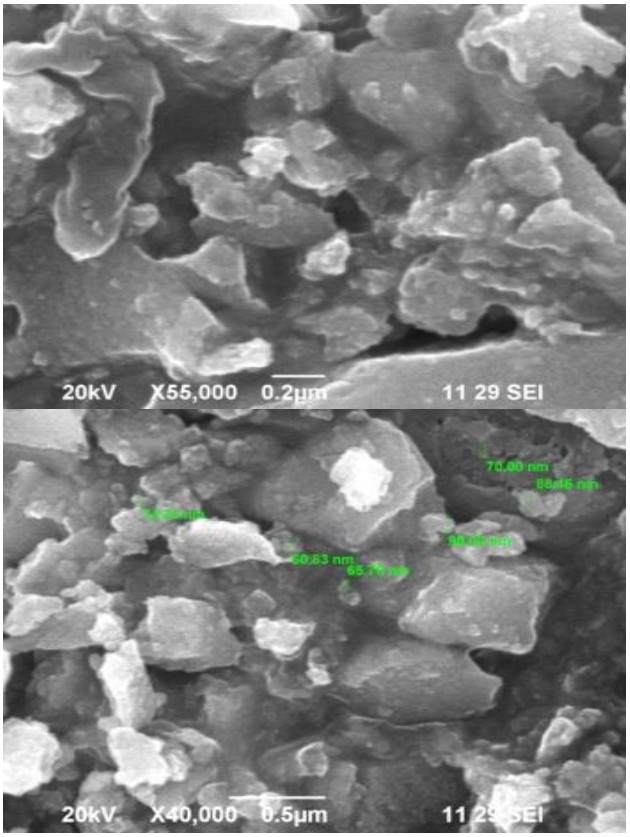

Fig. 3 (b): SEM images of Al-doped HAp nanoparticle

3.3 EDAX (Energy - Dispersive X-Ray Spectroscopy)

The elemental composition of the pure HAp and Al-doped HAp nanoparticles were carried out by EDAX spectroscopy. Fig. 4(a) and fig. (b) shows that the EDAX spectrum of pure and Al-doped Hap nanoparticles. The strong peaks observed in the spectrum of fig 3(a). related to Ca, P and O for pure. The prepared HAp nanoparticles have an atomic percentage of 72.25 of Oxygen, 9.84 of Phosphorus and 17.90 of Calcium. This confirmed the formation of Hap nanoparticles. The strong peaks observed in the spectrum of fig 3(b). related to Ca, P, O and Al for doped HAp. The prepared Al-doped HAp nanoparticles have an atomic percentage of 75.99 of Oxygen, 9.28 of Phosphorus, 13.69 of Calcium and 1.04 of aluminium. This is also confirmed the formation of Hap nanoparticles, and only a small amount of aluminium is present in the HAp lattice.

Table 3. The atomic content of the different type of Nanoparticles obtained from the EDAX measurements

Type of nanoparticles	EDAX results			
	Ca (at%)	P (at%)	O (at%)	Aluminium (at%)
Pure HAp	17.90	9.84	72.25	-
Al-doped HAp	13.69	9.28	75.99	1.04

3.4 FTIR Analysis

The FTIR spectrum of Pure and Al-doped HAp nanoparticles are heated at were recorded by using Perkin Elmer Spectrometer in the range of 400-4000 cm^{-1} using KBr pellet technique in order to identify the functional groups. In both of the spectrums are contains the broad peaks at 3432 cm^{-1} and 1642 cm^{-1} were attribute due to the absorbed water, while the sharp peak at 3368 cm^{-1} was attributable to the stretching vibrations of the lattice OH^- ions and the medium sharp peak at 633 cm^{-1} was assigned to the OH- deformation mode. The peak at 1636 cm^{-1} is assigned to the bending mode of water. The intense broad peak between 900 cm^{-1} and 1100 cm^{-1} is assigned to the stretching mode of PO_4^{3-}. The bending modes of PO_4^{3-} appeared at 602 cm^{-1} and 562 cm^{-1} as intense sharp peaks. The bands with a shoulder at 962 cm^{-1}-1105 cm^{-1} were assigned to the P-O stretching vibrations of the Phosphate groups. The weak band at about 470 cm^{-1} corresponds to the Phosphate bending vibration. The peak at 873 cm^{-1} is caused by HPO_4^{2-} groups. The CO_3^- derived bands are observed at 1402 cm^{-1} - 1460 cm^{-1}. It might be due to the absorption of an atmospheric Carbon-di-oxide during the sample preparation. The medium sharp peak at 902 cm^{-1} was assigned to Al-O stretching mode.

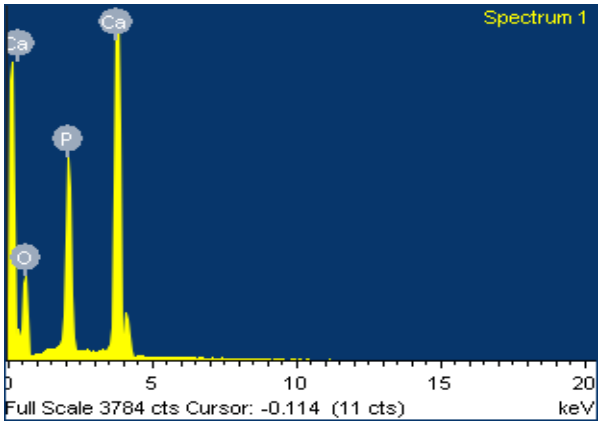

Fig. 4(a): Pure HAp

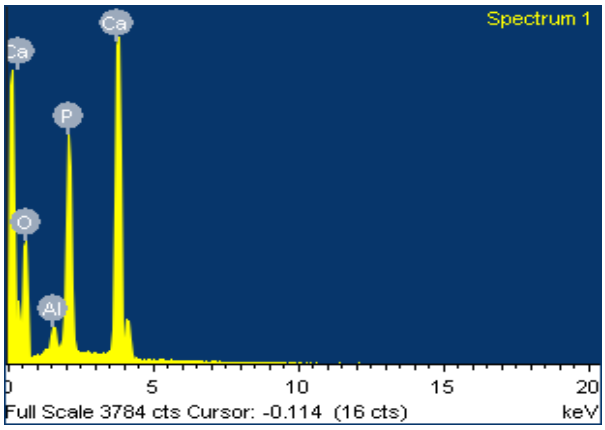

Fig. 4(b): Al-doped HAp

Table 4. Chemical functional groups assignments

Assignments	Functional groups cm^{-1}	
	Pure Hap (cm^{-1})	Al-doped Hap (cm^{-1})
OH –Stretching mode	3368	3415
H_2O – Bending mode	1646	1645
PO_4^{3-} - Stretching mode	1033	1041
PO_4^{3-} - Bending mode	565 & 602	565 & 603
PO - Stretching mode	962	963.85
PO - Bending mode	471	472
HPO_4^{2-}	873	875
Al-O - Stretching mode	-	901 cm^{-1}

The weak peak at 3570 cm^{-1} corresponds to the vibrations of OH^- ions in the HAp lattice. This indicates that the samples are good in the assigned mode. The table shows the functional groups assignments of pure HAp and Al-doped HAp nanoparticles.

3.5 Optical Studies

3.5.1 UV-Visible Studies

The optical behavior of the nanoparticles was assessed by using UV-Visible spectrometer instruments in the range of 200-1100 nm. An optical absorbance spectrum is shown in fig. 5(a) and (b). In the figure shows the UV-Visible spectra of pure and Al-doped HAp nanoparticles heated at 70˚C for 15 minutes. The lower cut off wavelength at 237.4 nm for pure HAp nanoparticles and 234.7nm for Al-doped HAp nanoparticles. It is indicated that the absorbance in the entire UV-Visible region of the spectrum. The bandgap energies are calculated using the formula:

$$E_v = h\gamma \qquad \text{i.e} \quad \gamma = c/\lambda$$
$$E_v = hc/\lambda$$

Where,

'h' is plank's constant i.e $h=6.626 \times 10^{-34} J/S$
'c' is Velocity of Light i.e $c= 3 \times 10^{8} m/s$
'λ' is Wavelength in nm

The bandgap energy for the spectra of pure HAp nanoparticles is 5.2eV. When the dopant. Al is added to the pure HAp nanoparticles the bandgap energy is slightly increased from 5.2eV to 5.3eV. This variation of bandgap energy is not affecting the conductivity. Because the small amount of dopant is added to the pure material. The absorption of the compound is due to the n-π^* transitions. Hence the compound may be useful for the fabrication of optical materials.

3.5.2 Photoluminescence Studies

The Photoluminescence spectrum occurs when the electron absorbs energy and is raised to an excited state. The excited state electrons are returns to the ground state by the emission of radiation. The Photoluminescence spectra for pure HAp nanoparticles and Al-doped HAp nanoparticles heated at 70˚C for 15 minutes were recorded using a Perkin Elmer LS45 model spectrometer in the range from 280 nm to 900.5 nm for pure HAp nanoparticles, and Al-doped HAp nanoparticles were observed in the spectrum of fig. 6 (a) and (b). The figure shows that the observed sharp emission Peaks at 529 nm for pure HAp nanoparticles and 530nm for Al-doped HAp nanoparticles. The pure HAp and Al-doped HAp nanoparticles spectrum indicate the emission of green light.

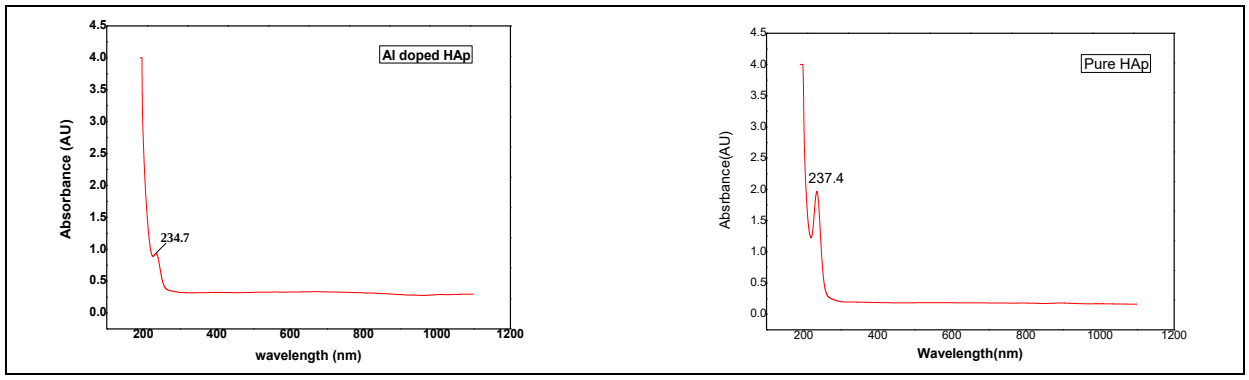

Fig. 5(a) & (b): UV spectrum of pure and Al-doped HAp nanoparticles

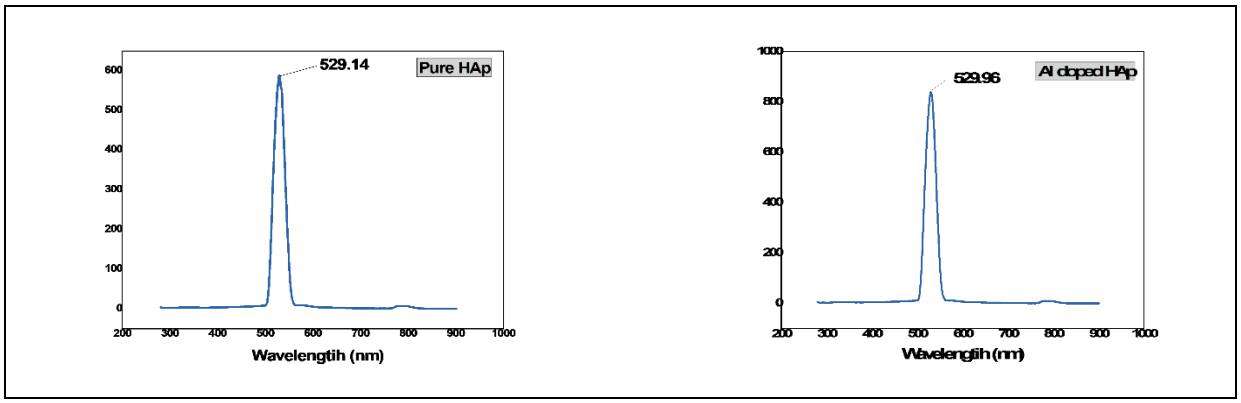

Fig. 6 (a) & (b): Photoluminescence spectra of Pure and Al-doped HAp nanoparticles

3.6 Antibacterial Studies

The agar well diffusion method was employed in antibacterial studies for prepared nanoparticles (Sriram *et al.* 2014). The antibacterial activity of the nanoparticles was tested against the gram-positive strains Staphylococcus aureus, gram-negative Escherichia Coli and gram-negative Staphylococcus epidermidis. The Zone of inhibition diameter values of the nanoparticles were determined and tabulated in Table 4.

Table 4. Zone of inhibition diameter of HAp nanoparticles (mm)

Strains	Zone of Inhibition diameter (mm)					
	Pure HAp		Al-doped HAp			
concentrations	75	100	25	50	75	100
Staphylococcus aureus	0	0	0	0	0	0
Escherichia Coli	4	5	0	0	3	5
Staphylococcus epidermidis	0	0	3	4	5	6

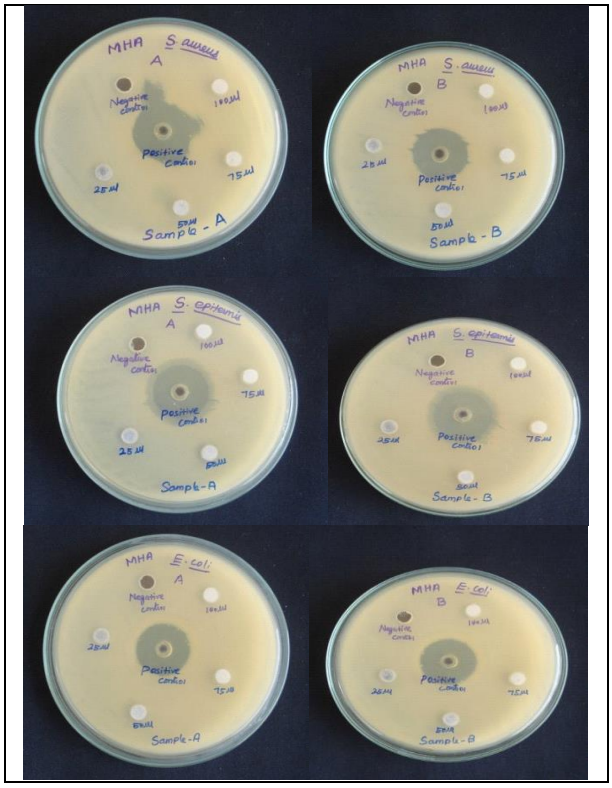

Fig. 7: Inhibition plates of Sample A – Pure HAp Sample B – Al-doped Hap

The zone of Inhibition diameter values were measured for four different concentrations (25, 50, 75 and 100 µg/ml). The bacterial inhibition was increased with increase in the concentration of nanoparticles (Fig.7). Staphylococcus aureus and Staphylococcus epidermidis were gram-positive bacterium. Escherichia Coli is a gram-negative bacterium. The pure HAp nanoparticles were effective on the gram-negative bacterium. The aluminium doped HAp nanoparticles were efficient on gram-positive bacterium of Staphylococcus epidermidis. The antibacterial effect of pure HAp nanoparticles was superior on Escherichia Coli than other strains.

The antibacterial effect of aluminium doped HAp nanoparticles was superior on Staphylococcus epidermidis than other strains. But gram-positive bacterium of Staphylococcus aureus is no activity on pure Hap and Al-doped Hap nanoparticles. In furthermore concentrations, it may be the effect on the bacteria. Thus HAp can be used for orthopedic applications.

4. CONCLUSION

Hydroxyapatite is the main biomaterial used in the field of orthopedic applications. Hydroxyapatite and Aluminium doped Hydroxyapatite nanoparticles were synthesized by microwave-assisted co-precipitation method. Biomaterials with aluminium dopant were applied for the present study in view of their bone replacement applications. The main proposition of this work is to synthesize the pure Hydroxyapatite and Aluminium doped Hydroxyapatite nanoparticles under room temperature. The prepared samples are characterized by using various techniques such as powder XRD, SEM, EDAX, UV-Visible, PL, and FT-IR method. The antimicrobial analysis was performed to study the in-vitro analysis of the samples. XRD reveals the crystalline size, Microstrain and dislocation density of the samples in the expected range. SEM reveals the spherical shaped morphology in both samples. The presence of Ca, P, O and Al under a proper proportion of 1.6 was revealed by EDAX, UV, and PL reveals the bandgap and excitation wavelength of the samples. Functional groups are determined by FTIR. Zone of inhibition for gram-positive and gram-negative bacteria was shown by antimicrobial analysis. Gram-negative bacteria have significant ZOI for all the samples. Thus we conclude Hydroxyapatite and Al-doped Hydroxyapatite can be applied as the best candidate for orthopedic applications.

REFERENCES

Amogh Tathe, M. G. A. A. P. N. *, A brief review: biomaterials and their apllication, *Int. J. Pharm. Pharm. Sci.* 2(4), 19–23 (2014).

Gopi, D., Indira, J., Kavitha, L., Sekar, M., Mudali, U. K., Synthesis of hydroxyapatite nanoparticles by a novel ultrasonic assisted with mixed hollow sphere template method, *Spectrochim. Acta Part A Mol. Biomol. Spectrosc.* 93, 131–134 (2012). https://dx.doi.org/10.1016/j.saa.2012.02.033

Kanimozhi, D. G. and L. K., Synthesis and characterization of banana peel derived biopolymer/hydroxyapatite nanocomposite for biomedical applications, *Int. J. Sci. Eng. Res.*, 5(3), 138 - 140(2014).

Kalaiselvi, V., Mathammal, R., Anitha, P., Synthesis and Characterization of Hydroxyapatite Nanoparticles using Wet Chemical Method, *Int. J. Adv. Sci. Eng.* 4(2), 571 (2017). https://dx.doi.org/10.29294/IJASE.4.2.2017.571-574

Sriram, T and Pandidurai, V., Synthesis of silver nanoparticles from leaf extract of Psidium guajava and its antibacterial activity against pathogens, *Int.J.Curr.Microbiol.App.Sci.*, 3(3), 146–152 (2014).

Rajendran, A., Barik, R. C., Natarajan, D., Kiran, M. S., Pattanayak, D. K., Synthesis, phase stability of hydroxyapatite–silver composite with antimicrobial activity and cytocompatability, *Ceram. Int.*, 40(7), 10831–10838 (2014). https://dx.doi.org/ 10.1016/j.ceramint.2014.03.075

Vignesh Raj, S., Rajkumar, M., Meenakshi Sundaram, N., Kandaswamy, A., Synthesis and characterization of hydroxyapatite/alumina ceramic nanocomposites for biomedical applications, *Bull. Mater. Sci.* 41(4), 93 (2018). https://dx.doi.org/10.1007/s12034-018-1612-4